phys. stat. sol. (b) **245**, No. 10, 2155–2158 (2008) / **DOI** 10.1002/pssb.200879612

physica status solidi b
www.pss-b.com
basic solid state physics

Coulomb effects in single-walled carbon nanotubes

Ermin Malić[1,*], Matthias Hirtschulz[1], Frank Milde[1], Marten Richter[1], Janina Maultzsch[2], Stephanie Reich[3], and Andreas Knorr[1]

[1] Institut für Theoretische Physik, Technische Universität Berlin, 10623 Berlin, Germany
[2] Institut für Festkörperphysik, Technische Universität Berlin, 10623 Berlin, Germany
[3] Fachbereich Physik, Freie Universität Berlin, 14195 Berlin, Germany

Received 30 April 2008, revised 9 June 2008, accepted 10 June 2008
Published online 29 August 2008

PACS 78.35.+c, 78.67.Ch

* Corresponding author: e-mail ermin@itp.physik.tu-berlin.de, Phone: +49-30-31423764, Fax: +49-30-314-21130

We present microscopic calculations of the excitonic absorption coefficient for single-wall carbon nanotubes. Our approach combines the density matrix formalism including the Coulomb and electron-light interaction with the tight-binding approximation. It allows the investigation of excitons in carbon nanotubes of arbitrary chiral index over a wide range of energy. We take all intra- and intersubband contributions into account and study the behavior of the Coulomb matrix elements for all relevant processes. The Coulomb interaction is found to decrease strongly with increasing momentum transfer perpendicular to the nanotube axis. Furthermore, we show that the band gap renormalization arising from the electron-electron interaction leads to a partial lifting of degeneracy in the spectra of zig-zag tubes.

1 Introduction Single-wall carbon nanotubes (CNTs) as prototypical one-dimensional structures have well defined optical properties. Hence, optical spectroscopy methods, such as absorption, photoluminescence, Rayleigh, and Raman scattering have become important characterization techniques for CNTs [1–4]. Theoretical investigations of free-particle band-to-band transitions have given good insight into their optical properties [5–10]. Three years ago, the optical excitations in CNTs were shown to be determined by excitons [11,12]. A number of theoretical investigations on excitonic properties have been performed by incorporating the Coulomb interaction within the Bethe-Salpeter equation combined with the GW method [13–17]. The carbon nanotubes Bloch equation (CNBE) approach [18] used in this work is based on the many-body density matrix theory [19,20]. The combination with the tight-binding (TB) wave functions allows the study of nanotubes of arbitrary chiral index. Furthermore, the inclusion of further interactions, such as exciton-phonon coupling or the consideration of nonlinear effects is straightforward [18, 21].

In this work, we focus on the importance of the Coulomb interaction when considering intersubband coupling with a momentum transfer perpendicular to the nanotube axis. Moreover, we investigate the effect of band gap renormalization caused by the electron-electron interaction.

2 Excitonic absorption coefficient The Hamilton operator of the CNT system consists of three parts $H = H_0 + H_{\text{el-light}} + H_{\text{Coul}}$. The free electron contribution is given by $H_0 = \sum_{\boldsymbol{l}} \varepsilon_{\boldsymbol{l}} a_{\boldsymbol{l}}^{+} a_{\boldsymbol{l}}$ with the single-particle energy $\varepsilon_{\boldsymbol{l}}$ calculated within the tight-binding approach [5,7,22,23]. We apply the formalism of the second quantization with the creation and annihilation operators $a_{\boldsymbol{l}}^{+}, a_{\boldsymbol{l}}$. The compound index $\boldsymbol{l}$ contains the band λ and the electronic wave vector $\boldsymbol{k}$. The second part of the Hamilton operator describes the electron-light interaction which is determined by the dot product of the vector potential $\boldsymbol{A}(t)$ and the optical matrix element $\boldsymbol{M}_{\boldsymbol{l},\boldsymbol{l}'}$ [6,8,18]: $H_{\text{el-light}} = i\frac{e_0\hbar}{m_0}\sum_{\boldsymbol{l},\boldsymbol{l}'} \boldsymbol{M}_{\boldsymbol{l},\boldsymbol{l}'} \cdot \boldsymbol{A}(t) a_{\boldsymbol{l}}^{+} a_{\boldsymbol{l}'}$. The third contribution is the Coulomb interactions $H_{\text{Coul}} = \frac{1}{2}\sum_{\boldsymbol{l}_1,\boldsymbol{l}_2,\boldsymbol{l}_3,\boldsymbol{l}_4} V_{\boldsymbol{l}_3,\boldsymbol{l}_4}^{\boldsymbol{l}_1,\boldsymbol{l}_2} a_{\boldsymbol{l}_1}^{+} a_{\boldsymbol{l}_2}^{+} a_{\boldsymbol{l}_3} a_{\boldsymbol{l}_4}$. The characteristics of the Coulomb matrix elements $V_{\boldsymbol{l}_3,\boldsymbol{l}_4}^{\boldsymbol{l}_1,\boldsymbol{l}_2}$ are discussed in the next section.

Starting with the Hamilton operator we can calculate the absorption coefficient $\alpha(\omega)$ which is given by the imaginary part of the optical susceptibility [8]:

$$\alpha(\omega) \propto \omega Im\chi(\omega) = -\frac{2e_0\hbar}{m_0\varepsilon_0}\sum_{\boldsymbol{k}}\frac{Re[M_z^{cv}(\boldsymbol{k})p_{\boldsymbol{k}}(\omega)]}{\omega A(\omega)} \quad (1)$$

with m_0 as the bare electron mass, e_0 as the elementary charge, and $c(v)$ labelling conduction (valence) band. The response function $\chi(\omega)$ is calculated within the density matrix theory by deriving the optical Bloch equation for the microscopic polarization $p_{\boldsymbol{k}}(t) = \langle a^+_{v,\boldsymbol{k}} a_{c,\boldsymbol{k}}\rangle$. The latter expresses the probability amplitude for an optical transition at the wave vector $\boldsymbol{k}$. Only the z-component of the optical matrix element $M_z^{cv}(\boldsymbol{k})$ is taken into account since we only consider z-polarized light (along the nanotube axis) accounting for the depolarization effect that strongly suppresses light polarized perpendicular to the nanotube axis [24]. To determine the matrix elements we describe the electronic single-particle wave functions of carbon nanotubes within the TB approach combined with the zone-folding approximation [5,22]. The periodic boundary conditions around the nanotube circumference are considered by restricting the allowed wave vectors $\boldsymbol{k}$ to lines in the graphene Brillouin zone $\boldsymbol{k} = (k_z, m)$ with m as the subband index. Using the Heisenberg equation of motion we derive the carbon nanotube Bloch equation (CNBE) [18]:

$$\dot{p}_{\boldsymbol{k}}(t) = -i\Delta\omega_{\boldsymbol{k}} p_{\boldsymbol{k}}(t) + g_{\boldsymbol{k}}(t) - \gamma p_{\boldsymbol{k}}(t)\,. \quad (2)$$

The microscopic polarization $p_{\boldsymbol{k}}(t)$ is determined by the renormalized band transition frequency

$$\Delta\omega_{\boldsymbol{k}} = [\omega_c(\boldsymbol{k}) - \omega_v(\boldsymbol{k})] - \frac{i}{\hbar}\sum_{\boldsymbol{k}'} V_{ren}(\boldsymbol{k},\boldsymbol{k}') \quad (3)$$

and the excitonic Rabi frequency

$$g_{\boldsymbol{k}}(t) = \frac{e_0}{m_0} M_z^{cv}(\boldsymbol{k})A(t) - \frac{i}{\hbar}\sum_{\boldsymbol{k}'} V_{exc}(\boldsymbol{k},\boldsymbol{k}')p_{\boldsymbol{k}'}\,. \quad (4)$$

The damping parameter γ describes the dephasing resulting from electron-phonon coupling or other neglected interactions. Its value $\gamma = (0.0125/\hbar)$eV [8] determines the linewidth in the calculated spectra, but has no influence on the position of the peaks.

The evaluation of Eq. (1) yields excitonic absorption spectra for nanotubes with arbitrary chiral index. Figure 1 shows the spectra of the (8,4) chiral nanotube illustrating the different contributions to the microscopic polarization discussed above. The free electron spectra are characterized by the Van Hove singularity. Including the renormalization of the band gap due to the electron-electron interaction leads to a large blue shift. The reduction in intensity arises from the ω^{-1} dependence of the absorption coefficient (see Eq. (1)). After including the electron-hole coupling the renormalized Van Hove singularity is red-shifted and reshaped to a Lorentzian resulting in a net blue-shift. The excitonic binding energy of 0.7eV (with the dielectric constant $\varepsilon_{bg} = 1$) can be easily determined as the difference between the peak with and without electron-hole coupling.

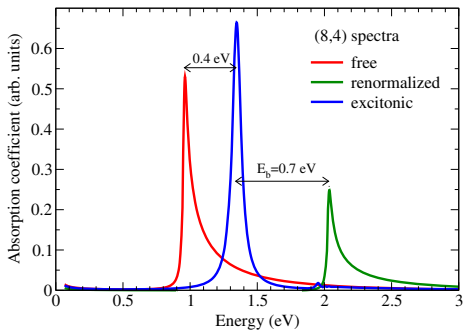

Figure 1 Absorption spectra of the (8,4) nanotube (for reasons of clarity only the first transition E_{11} is shown). Coulomb interaction leads to 1) band gap renormalization due to the electron-electron coupling (blue shift of the Van Hove singularity) and 2) formation of excitons due to the electron-hole interaction (red-shift of the renormalized Van Hove singularity and reshaping into an Lorentzian), see also [18].

The equations (3),(4) contain the Coulomb contributions $V_{\rm ren} = V^{c\boldsymbol{k},v\boldsymbol{k}'}_{v\boldsymbol{k}',c\boldsymbol{k}} - V^{v\boldsymbol{k}',v\boldsymbol{k}}_{v\boldsymbol{k},v\boldsymbol{k}'}$ and $V_{\rm exc} = V^{c\boldsymbol{k},v\boldsymbol{k}'}_{c\boldsymbol{k}',v\boldsymbol{k}} - V^{c\boldsymbol{k},v\boldsymbol{k}'}_{v\boldsymbol{k},c\boldsymbol{k}'}$ that determine the band gap renormalization and the formation of excitons, respectively. In the following section, we discuss the characteristics of the Coulomb matrix elements in more detail.

3 Coulomb matrix element The Coulomb matrix elements $V^{l_1,l_2}_{l_3,l_4}$ are calculated within the tight-binding approximation. Applying the TB single-particle wave functions $\Psi^{c,v}(\boldsymbol{k},\boldsymbol{r}) = \sum_{j=A,B} C^{c,v}_j(\boldsymbol{k})\phi_j(\boldsymbol{k},\boldsymbol{r})$ as a linear combination of the Bloch functions $\phi_j(\boldsymbol{k},\boldsymbol{r})$ consisting of two atoms A and B in the graphene unit cell yields

$$V^{l_1,l_2}_{l_3,l_4} = \sum_{i,j=A,B} C^{i*}_{\boldsymbol{l_1}} C^{j*}_{\boldsymbol{l_2}} C^{i}_{\boldsymbol{l_3}} C^{j}_{\boldsymbol{l_4}} V^{ij}(\boldsymbol{q})\delta_{l_3-l_1,l_4-l_2}\,, \quad (5)$$

with the tight-binding coefficient functions $C^i_{l_1}$ where $\boldsymbol{l}_1$ is a compound index containing the band index $\lambda = c,v$ and the wave vector $\boldsymbol{k}_1 = (k^z_1, m)$. The conservation of the momentum is expressed by the Kronecker delta δ. The Fourier transform of the Coulomb potential is given by

$$V^{ij}(\boldsymbol{q}) = \frac{1}{N}\sum_l e^{i\boldsymbol{q}\cdot(\boldsymbol{R}^i_l - \boldsymbol{R}^j_0)} V^{ij}(|\boldsymbol{R}^i_l - \boldsymbol{R}^j_0|)\,, \quad (6)$$

with the lattice vectors $\boldsymbol{R}^i_l$, the normalization factor N, and the momentum transfer $\boldsymbol{q} = \boldsymbol{k}_3 - \boldsymbol{k}_1 = (q_z, \Delta m)$. The Coulomb interaction in one-dimensional structures needs to be treated with care since the ground state is known to have an infinite energy [25]. This problem can be avoided by introducing a regularized Coulomb potential that takes into account that CNTs are not strictly one-dimensional. In

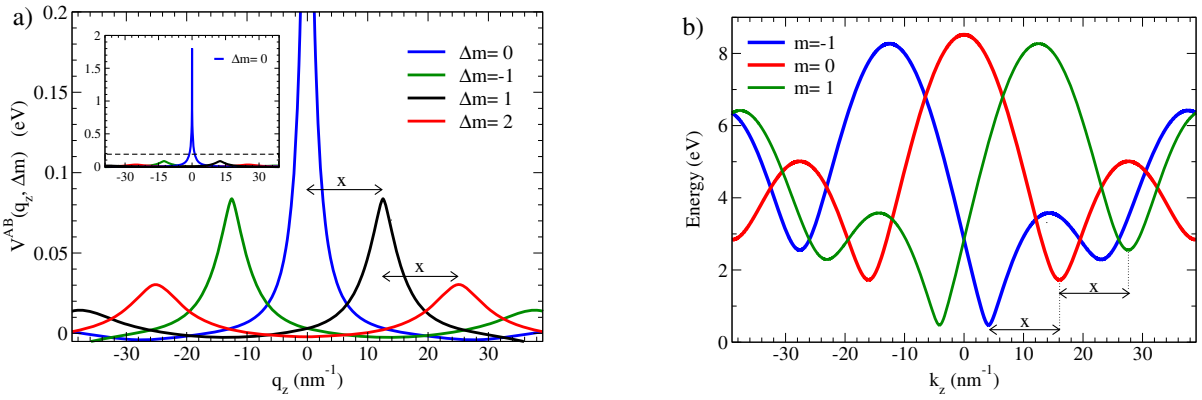

Figure 2 a) The inset shows the Fourier transform of the Coulomb potential $V^{AB}(q_z,\Delta m)$ for the (8,4) tube as a function of the momentum transfer q_z along the nanotube axis ($V^{AA}(q_z,\Delta m)$ shows a similar behavior). The region marked with a dashed line in the inset is plotted as a blow-up in the main figure showing the Coulomb contribution which arises from processes with a momentum transfer perpendicular to the nanotube axis, i.e. $\Delta m \neq 0$. b) The band structure of the (8,4) tube shows that the distance x between the band minima exactly corresponds to the relative maxima of the Coulomb interaction $x = \frac{r}{n}\frac{2\pi}{a}$ in Fig. 2a.

this work the unscreened Coulomb interaction $V^{ij}(|\boldsymbol{R}_l^i - \boldsymbol{R}_0^j|)$ in Eq. (6) is parametrized by the Ohno potential which has already been shown to be a good approximation for CNTs [14, 15, 17].

Having a line group symmetry nanotubes can be described with helical or roto-translational (linear) quantum numbers [26, 22]. Our calculations are performed with the helical quantum numbers having the advantage that no Umklapp rules need to be taken into account when the boundary of the Brillouin zone (BZ) or the Γ point is crossed. Note, that for an accurate description of excitonic effects (chirality and family behavior), it is necessary to consider the full (helical) BZ, especially for chiral nanotubes with large unit cells. The transformation between the linear $(\tilde{k}_z,\tilde{m})$ and helical indices (k_z,m) is given by $(k_z,m) = (\tilde{k}_z + \tilde{m}\frac{r}{n}\frac{2\pi}{a} + K\frac{q}{n}\frac{2\pi}{a}, \tilde{m} + Mn)$ with K and M as integers used to assure that the momenta are from the intervals $k_z \in (-\frac{q}{n}\frac{\pi}{a}, \frac{q}{n}\frac{\pi}{a}]$, $m \in (-\frac{n}{2}, \frac{n}{2}]$ with q as the number of hexagons in a nanotube unit cell, a as the unit cell length and n as the greatest common divisor of (n_1,n_2) [26]. The Fourier transformation of the Coulomb potential $V^{ij}(\boldsymbol{q})$ in Eq. (5) is performed atom-wise using the line group symmetry operations that allow us to construct an entire nanotube starting from a single carbon atom at the position $\boldsymbol{r}_{000}$: $\boldsymbol{r}_{tsu} = (C_q^{rt}C_n^s U^u|tna/q)\boldsymbol{r}_{000}$ with the pure rotations C_n^s $(s = 0,1,...,n-1)$, the U operation mapping atom A to atom B $(u = 0,1)$, and screw axis rotation $(C_q^{rt}|tna/q)$ (combination of rotations and translations with $t = 1 - q/2n, ..., q/2n$) [22]. This way we can distinguish between the two atoms A and B where $V^{AA}(\boldsymbol{q}) = V^{BB}(\boldsymbol{q})$ and $V^{AB}(\boldsymbol{q}) = V^{BA*}(\boldsymbol{q})$.

Figure 2a) shows the Fourier transform of the Coulomb potential as a function of the momentum transfer q_z along the nanotube axis for processes with $\Delta m = 0$ and $\Delta m \neq 0$. The Coulomb interaction reaches the maximal value when the involved electrons have the same momentum, i.e. for processes with $\Delta m = 0$ and $q_z = 0$. The second maxima is found for $\Delta m = 1$ at $q_z = \frac{r}{n}\frac{2\pi}{a}$, i.e. for transitions between two energetically neighboured subbands. For this process, the Coulomb interaction is strongly enhanced when a momentum of $q_z = \frac{r}{n}\frac{2\pi}{a}$ is carried over along the nanotube axis. This corresponds to a transition between the subband minima (see Fig. 2b). However, the coupling strength decreases strongly with increasing momentum transfer perpendicular to the nanotube axis, e.g. the Coulomb interaction for the process with $\Delta m = 1$ ($\Delta m = 2$) is less than 5% ($< 2\%$) of the absolute maxima for $\Delta m = 0$.

4 Band gap renormalization The Fourier transform of the Coulomb potential is a direct measure for the strength of Coulomb effects, such as the band gap renormalization (cp. Eq. (3))

$$V_{ren}(\boldsymbol{k},\boldsymbol{k}') = Re\left[\frac{e^*(\boldsymbol{k}')e(\boldsymbol{k})}{|e(\boldsymbol{k}')e(\boldsymbol{k}')|}V^{AB}(q_z,\Delta m)\right] \qquad (7)$$

with $q_z = k_z' - k_z$ and $\Delta m = m' - m$. Eq. (7) has been calculated using the expressions for the nearest neighbor tight-binding coefficients $C_B = \frac{1}{\sqrt{2}}$ and $C_A^{c,v}(\boldsymbol{k}) = \mp C_B\frac{e(\boldsymbol{k})}{|e(\boldsymbol{k})|}$ with the abbreviation $e(\boldsymbol{k}) = \sum_{j=1}^{3}\exp[i\boldsymbol{k}\cdot(\boldsymbol{R}_j - \boldsymbol{R}_0)]$ where $\boldsymbol{R}_j$ are the lattice vectors of the three nearest neighbor atoms [8]. The contribution $V_{ren}(\boldsymbol{k},\boldsymbol{k}')$ is illustrated in Fig. 1 in the case of the (8,4) nanotube. The free-particle energy is renormalized by 1.1eV that is about 100% of the free band gap which is a sign for the strong Coulomb interaction in carbon nanotubes.

In an earlier work [8] we have shown that (n,0) zig-zag nanotubes with n even have a pronounced peak at higher energies which dominates the overall intensity in their absorption spectra. We explained this effect by showing that within the tight-binding approximation the mentioned zig-

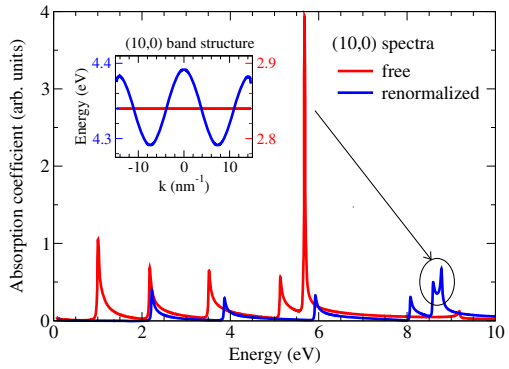

Figure 3 Illustration of the importance of the band gap renormalization. The dispersionless band with m=5 gains a small oscillating dispersion after electron-electron coupling is included (shown in the inset). As a result, the pronounced peak with the high intensity splits up into two peaks with a similar coupling strength.

zag tubes have a dispersionless band with $\tilde{m} = n/2$ leading to a formally infinite density of states. Additionally, a degeneracy with the band $\tilde{m} = n$ further increases the intensity of the peak. However, Coulomb effects change the dispersion of the band $\tilde{m} = n/2$ (see the renormalized band structure in the inset of Fig. 3). This results in a finite density of states and a much smaller intensity of the corresponding peak. Moreover, the gain of dispersion also account for the lifting of the mentioned degeneracy with the band $\tilde{m} = n$ leading to a peak splitting shown in Fig. 3. A similar effect can be observed in the spectra of other nanotubes where the energy renormalization often enlarges the distance between peaks. As a result, energetically close transitions can be resolved in the spectra.

5 Conclusions In conclusion, we presented a method to calculate the excitonic absorption coefficient for arbitrary carbon nanotubes within the density matrix formalism combined with tight-binding single-particle wave functions. The Coulomb matrix elements are shown to be maximal when the momentum transfer along and perpendicular to the nanotube axis is low. Processes around $q_z = 0$ and with $\Delta m = 0$ give the maximal contribution to the Coulomb interaction. For processes with a perpendicular momentum transfer, i.e. $\Delta m \neq 0$, the coupling strength is reduced to less than 5%. Furthermore, we found that the band gap renormalization arising from the electron-electron interaction leads to a partial lifting of degeneracy in (n,0) zigzag tubes with n even. As a result, the pronounced peak in the absorption spectra of these tubes splits up into two peaks with a similar intensity.

Acknowledgements We thank DPG for support via the center of excellence UNICAT. E. M. is grateful to *Studienstiftung des deutschen Volkes* for financial support.

References

[1] S. M. Bachilo, M. S. Strano, C. Kittrell, R. H. Hauge, R. E. Smalley, and R. B. Weisman, Science **298**, 2361 (2002).
[2] C. Fantini, A. Jorio, M. Souza, M. S. Strano, M. S. Dresselhaus, and M. A. Pimenta, Phys. Rev. Lett. **93**, 147406 (2004).
[3] M. Y. Sfeir, F. Wang, L. Huang, C. C. Chuang, J. Hone, S. P. O'Brien, T. F. Heinz, and L. E. Brus, Science **306**, 1540 (2004).
[4] Y. Miyauchi, S. Chiashi, Y. Murakami, Y. Hayashida, and S. Maruyama, Chem. Phys. Lett. **387**, 198 (2004).
[5] R. Saito, G. Dresselhaus, and M. S. Dresselhaus, Phys. Rev. B **61**, 2981 (2000).
[6] A. Grüneis, R. Saito, G. G. Samsonidze, T. Kimura, M. A. Pimenta, A. Jorio, A. G. SouzaFilho, G. Dresselhaus, and M. S. Dresselhaus, Phys. Rev. B **67**, 165402 (2003).
[7] V. N. Popov and L. Henrard, Phys. Rev. B **70**, 115407 (2004).
[8] E. Malić, M. Hirtschulz, F. Milde, A. Knorr, and S. Reich, Phys. Rev. B **74**(19), 195431 (2006).
[9] E. Malić, M. Hirtschulz, F. Milde, Y. Wu, J. Maultzsch, T. F. Heinz, A. Knorr, and S. Reich, phys. stat. sol. (b) **244**(11), 4240 (2007).
[10] E. Malić, M. Hirtschulz, F. Milde, Y. Wu, J. Maultzsch, T. F. Heinz, A. Knorr, and S. Reich, Phys. Rev. B **77**(4), 045432 (2008).
[11] F. Wang, G. Dukovic, L. E. Brus, and T. F. Heinz, Science **308**, 838 (2005).
[12] J. Maultzsch, R. Pomraenke, S. Reich, E. Chang, D. Prezzi, A. Ruini, E. Molinari, M. S. Strano, C. Thomsen, and C. Lienau, Phys. Rev. B **72**, 241402(R) (2005).
[13] C. D. Spataru, S. Ismail-Beigi, L. X. Benedict, and S. G. Louie, Phys. Rev. Lett. **92**, 077402 (2004).
[14] V. Perebeinos, J. Tersoff, and P. Avouris, Phys. Rev. Lett. **92**, 257402 (2004).
[15] H. Zhao and S. Mazumdar, Phys. Rev. Lett. **93**, 157402 (2005).
[16] R. B. Capaz, C. D. Spataru, S. Ismail-Beigi, and S. G. Louie, Phys. Rev. B **74**(12), 121401 (2006).
[17] J. Jiang, R. Saito, G. G. Samsonidze, A. Jorio, S. G. Chou, G. Dresselhaus, and M. S. Dresselhaus, Phys. Rev. B **75**(3), 035407 (2007).
[18] M. Hirtschulz, F. Milde, E. Malić, S. Butscher, C. Thomsen, S. Reich, and A. Knorr, Phys. Rev. B **77**(3), 035403 (2008).
[19] M. Lindberg and S. W. Koch, Phys. Rev. B **38**(5), 3342 (1988).
[20] F. Rossi and T. Kuhn, Rev. Mod. Phys. **74**(3), 895 (2002).
[21] S. Butscher, F. Milde, M. Hirtschulz, E. Malić, and A. Knorr, Appl. Phys. Lett. **91**(20), 203103 (2007).
[22] S. Reich, C. Thomsen, and J. Maultzsch, Carbon Nanotubes: Basic Concepts and Physical Properties (Wiley-VCH, Berlin, 2004).
[23] S. Reich, J. Maultzsch, C. Thomsen, and P. Ordejón, Phys. Rev. B **66**, 035412 (2002).
[24] H. Ajiki and T. Ando, J. Phys. Soc. Jpn. **62**, 4267 (1993).
[25] R. Loudon, Am. J. Phys. **27**, 649 (1959).
[26] M. Damnjanović, I. Milosević, T. Vuković, and J. Maultzsch, J. Phys. A **36**(21), 5707 (2003).

